THE ASTRONOMICAL JOURNAL VOLUME 104, NUMBER 5 NOVEMBER 1992

SYMPLECTIC MAPS FOR THE n-BODY PROBLEM: STABILITY ANALYSIS

JACK WISDOM AND MATTHEW HOLMAN

Department of Earth, Atmospheric, and Planetary Sciences, Massachusetts Institute of Technology, Cambridge, Massachusetts 02139

Received 10 April 1992; revised 1 June 1992

ABSTRACT

The stability of the symplectic mapping method for the n-body problem introduced recently by Wisdom & Holman [AJ, 102, 1528 (1991)] is analyzed in a novel application of the methods of nonlinear dynamics.

1. INTRODUCTION

We recently introduced a new symplectic mapping method for studying the long term evolution of n-body problems with a dominant central mass (Wisdom & Holman, 1991, hereafter WH91). The method shows promise of being a valuable tool in the numerical exploration of planetary and satellite n-body systems. Tests of the method in various problems have indicated that the new mapping method can be an order of magnitude faster than other methods of numerical integration. It has already been used to carry out record-breaking, long-term integrations of the solar system. In particular, Sussman & Wisdom (1992) used the mapping method to integrate the whole solar system for 100 million years. This integration confirmed the result of Laskar (1990) that the evolution of the solar system is chaotic with a surprisingly short timescale for exponential divergence of only 4 million years. In this paper, we examine more carefully the dynamical mechanisms which govern the stability of the mapping method. Our goal is to clarify the regime of applicability and understand more clearly the limitations of the mapping method.

We present here a novel technique for analyzing the nonlinear stability of a numerical integration technique. The mapping is derived as the time evolution of a Hamiltonian. We analyze the mapping Hamiltonian as we would any other dynamical system using the tools of nonlinear dynamics. The true Hamiltonian and the mapping Hamiltonian differ by the addition of a suite of resonances associated with the mapping stepsize. The evolution computed with the mapping approximates the true evolution provided these stepsize resonances do not significantly affect the evolution. We identify the principal stepsize resonances and analyze each in detail. Gross instability of the mapping method is associated with overlap of the principal stepsize resonances.

2. MAPPING METHOD

The mapping method is a generalization of the resonance mapping method of Wisdom (1982, 1983). The derivation of the mapping method is detailed in WH91. Briefly, the Hamiltonian for the n-body problem can be written

$$H = H_{\rm Kepler} + H_{\rm Interaction}, \tag{1}$$

where $H_{\rm Kepler}$ represents the basic Keplerian motion of each of the planets around the dominant central mass, and $H_{\rm Interaction}$ represents the interactions among them. Elimination of the center of mass may be accomplished by using Jacobi coordinates or canonical heliocentric coordinates. There is considerable freedom in deriving maps; see WH91 for details. The mapping method is based on the averaging principle: rapidly varying terms do not contribute significantly to the long-term evolution. Thus rapidly varying terms can be added or subtracted from the Hamiltonian with impunity. The simplest mapping is obtained by introducing extra high-frequency terms through periodic delta functions

$$H_{\rm Map} = H_{\rm Kepler} + 2\pi\delta_{2\pi}(\Omega t) H_{\rm Interaction}, \tag{2}$$

where $\delta_{2\pi}(t)$ is a periodic sequence of Dirac delta functions with period 2π, and Ω is the mapping frequency. The time between delta functions is the stepsize $h = 2\pi/\Omega$. The delta functions have the Fourier representation

$$\delta_{2\pi}(t) = \frac{1}{2\pi} \sum_{l=-\infty}^{\infty} \cos(lt). \tag{3}$$

Multiplying the interaction part of the Hamiltonian by the periodic delta function gives the original interaction Hamiltonian plus the same terms multiplied by terms of high frequency. The average of the mapping Hamiltonian over a mapping period gives the original n-body Hamiltonian. The advantage of introducing the delta functions is that the mapping Hamiltonian is locally integrable: Between the delta functions each planet evolves along an unperturbed Keplerian orbit, and, also, the system is trivially integrated across the delta functions since the interaction Hamiltonian can be written solely in terms of the Cartesian coordinates. For the map to be a viable numerical method it is essential to be able to rapidly advance Keplerian orbits, and minimize intermediate canonical transformations. We eliminate the need for intermediate transformations by using Cartesian coordinates throughout; Keplerian orbits can be rapidly advanced directly in Cartesian coordinates using Gauss' f and g functions. Several extensions of the mapping method are presented in WH91.

 0004-6256/92/112022-08$00.90

3. OVERVIEW OF NONLINEAR STABILITY

Traditionally, the stability of an integrator is analyzed by applying the integrator to a linear system, and then solving the resulting set of linear difference equations. The linear stability of the method is then hoped to be relevant to the stability of the method when it is applied to the integration of nonlinear problems. There is really no other choice, because the system of nonlinear difference equations obtained in the approximation of a nonintegrable dynamical system are too complicated to tackle directly. The Hamiltonian nature of the mapping offers a tremendous advantage for stability analysis. It allows us to study the nonlinear stability of our mapping method using the usual tools of Hamiltonian dynamics. For background on Hamiltonian dynamics see, for example, Chirikov (1979) and Lichtenberg & Lieberman (1983).

An analogy will help clarify the following stability analysis. Let us construct a simple mapping for the mathematical pendulum

$$H=\tfrac{1}{2}p^2+\epsilon\cos\theta. \tag{4}$$

According to our usual procedure we introduce a periodic sequence of delta functions into the "perturbation" part of the Hamiltonian (ignoring and, in fact, destroying the integrability of the original system)

$$H_{\rm Map}=\tfrac{1}{2}p^2+2\pi\delta_{2\pi}(\Omega t)\epsilon\cos\theta. \tag{5}$$

This Hamiltonian is locally integrable: we easily compute the momentum change as the system crosses a delta function, and between the delta functions the angle rotates uniformly. The resulting map is

$$p'=p+\frac{2\pi}{\Omega}\epsilon\sin\theta, \tag{6}$$

$$\theta'=\theta+p'\frac{2\pi}{\Omega}. \tag{7}$$

Higher order versions of this map could easily be constructed, as described in WH91. This map is a simple finite difference approximation to the evolution of the pendulum. As a consequence of being derived from a Hamiltonian, this finite difference scheme is symplectic, which in this case simply means it is area preserving. So we have a first-order symplectic integrator for the pendulum. The stepsize, or mapping step, is $h=2\pi/\Omega$. In terms of the scaled momentum $I=ph$, and the parameter $K=h^2\epsilon$, the map takes the form

$$I'=I+K\sin\theta, \tag{8}$$

$$\theta'=\theta+I'. \tag{9}$$

We furthermore note that the dynamics is unchanged if we write the map in terms of a shifted momentum $J=I+2\pi n$, where n is some integer. Thus, without any loss of dynamical possibilities we can consider the momentum to be periodically wrapped through the interval 0 to 2π, i.e., the momentum can be considered to be an angle variable. This is now the usual standard map (Chirikov 1979). In the context of this paper though it is clearer to not restrict the momentum to be an angle. This identification of the standard map as a symplectic finite difference approximation to the pendulum is well known (see, for example, Sanz-Serna & Vadillo 1986).

The behavior of the standard map has been the object of a tremendous number of investigations, both mathematical and numerical. In the present context the review of Chirikov (1979) is most relevant. Though much is known about its behavior, it is not likely ever to be exhaustively understood. In what sense then does the standard map approximate the pendulum? Let us review the gross behavior of the standard map from this point of view.

The standard map exhibits a gross transition to large scale chaos roughly for $K>1$. In that regime the dynamics has little to do with the pendulum. For small values of the parameter K (equivalently small mapping stepsize h) the phase space of the standard map displays a single pendulum-like resonance centered at $I=p=0$, as well as periodic copies of this resonance, as described above, spaced by $\Delta I=2\pi$ (equivalently $\Delta p=\Omega$). As long as we avoid the phase space near the periodic copies of our basic pendulum resonance the most notable departure of the mapping approximation to the pendulum from the pendulum itself is the appearance of a chaotic zone near the pendulum separatrix. The size of this chaotic zone has been estimated by Chirikov using the resonance overlap criterion. The resonances which overlap are the resonances between the libration period of the pendulum and the mapping period. There is an accumulation of these resonances as the unstable equilibrium is approached because the libration period of the pendulum diverges and as it diverges it successively matches every multiple of the mapping period. For our mapping approximation to the pendulum, application of the Chirikov formula for the width of the separatrix yields

$$\Delta\theta=\frac{8\pi^2}{h^{3/2}\epsilon^{3/4}}\exp\left(-\frac{\pi^2}{2h\epsilon^{1/2}}\right), \tag{10}$$

where $\Delta\theta$ is the half-width in θ of the chaotic zone near the unstable equilibrium. For small stepsizes h the size of this unwanted chaotic zone decreases very rapidly, as $\exp(-c/h)$. For example, even if we take only 10 mapping steps per small amplitude libration period of the pendulum (the natural timescale), the unwanted chaotic zone has a fractional width of only about one percent. With 50 steps per libration period the size of the chaotic zone is reduced to less than one part in 10^{14}. If we are not interested in this particular region of the phase space, it is easy to avoid. In general, we are interested in some particular finite amplitude oscillation of the pendulum. The mapping will become grossly unstable for this particular trajectory if a stepsize h is chosen for which the chaotic zone near the separatrix is so large that the trajectory is engulfed in it. This clearly depends on the particular trajectory of interest; the closer the trajectory is to the separatrix the smaller the stepsize has to be to avoid this gross instability.

There are other artifacts introduced by the mapping approximation. From the Poincare–Birkhoff theorem we expect there are an infinite set of islands in the phase space

of the standard map. Whenever the libration frequency is commensurate with the mapping frequency a chain of alternating stable and unstable periodic orbits appears in the phase space. Since the rationals are dense, the secondary islands associated with the stable periodic orbits are dense in the phase space. Of course these islands do not exist in the original pendulum problem. These islands however do not give rise to significant artifacts; they are generally extremely small. Only by extreme bad luck would the trajectory of interest, with an arbitrarily chosen stepsize, fall on one of these islands. We must, however, keep in mind this possible artifact. For example, each of these secondary unstable points is associated with its own chaotic zone. If we are calculating the Lyapunov exponent for our system, we should consider the possibility that by chance we fell into one of these chaotic zones introduced by the mapping approximation.

We can say more clearly what it means for the mapping method to be nonlinearly stable. If we could prove that the trajectory as computed by the map is an invariant curve or is bound in the phase space by invariant curves, then the trajectory will always remain just as far from the pendulum orbit as it was in the beginning. Of course, this is extremely difficult to do. The Kolmogorov–Arnold–Moser theorem proves that near the stable fixed point of the pendulum map that most of the invariant curves (with given frequency) of the pendulum are preserved in the mapping approximation. The exceptions are those which are too near the Poincare–Birkhoff islands, but these are of small measure. What happens at larger distances from the stable fixed point? Though it is not proven, numerical experiments suggest that the phase space is still dominated by invariant curves. One possibility, however, is that the invariant curves are actually cantori with small holes through which the mapping trajectory can ultimately leak out (Percival 1979). Thus to prove the nonlinear stability of the method for a particular trajectory for a particular stepsize, one must prove either that the trajectory is an invariant curve or that it is bounded by invariant curves rather than cantori. Practically though, the islands appear to behave as though most of the trajectories in them are invariant curves. An exception might be if the trajectory is very close to the edge of the island, for then the timescale to leak through the cantori may be comparable to the timescale of interest in the numerical experiment, but if the trajectory is close to the edge of the island then the stepsize has been chosen so that the mapping method is very close to the border of instability, as discussed above. This situation is easy to avoid, by choosing a better stepsize.

For systems with many degrees of freedom, the question of stability is much more complicated, principally because trajectories of the actual system can now be chaotic. We must consider what stability would mean for both quasiperiodic and chaotic trajectories. For quasiperiodic trajectories the situation is similar to the single degree-of-freedom case. If the mapping trajectory can be proven to lie on an invariant curve that remains close to the true invariant curve of the original system then the method can be declared to be stable. Of course, if we could prove these things we would not be using a mapping approximation to study the system. With two degrees of freedom, if the mapping trajectory is chaotic, but bound close to the true trajectory by invariant curves, then the mapping can be said to be stable. With many degrees of freedom, it is conjectured that all chaotic zones are connected (the "Arnold web") and that Arnold diffusion eventually carries the trajectory everywhere along it. Practically speaking though the Arnold diffusion is usually extremely slow, and the connectedness of the chaotic zones is often ignorable. Thus even if the mapping trajectory corresponding to a quasiperiodic trajectory of the modeled system is chaotic, because for instance that it fell on one of the chaotic zones associated with one of the Poincare–Birkhoff unstable periodic orbits, we may still think of the mapping method as stable provided the computed trajectory stays near the actual trajectory for the duration of the numerical experiment. Of course the small positive Lyapunov exponent of the computed trajectory must be recognized as an artifact. It is also possible for the actual trajectory of the system to be chaotic. Stability of the mapping method in this case means that any quantity which characterizes the chaotic zone in which the trajectory moves is accurately reproduced by the mapping approximation. For example, it should be the case that the size and shape of the chaotic zone are well reproduced, as well as the Lyapunov exponent. It would not be expected that individual trajectories of the actual system and the map are the same. Rather, shadowing results suggest that computed trajectories approximate real trajectories of the original system, though they do not approximate trajectories which can be specified *a priori* (Grebogi *et al.* 1990). We have argued that maps make sense from the point of view of averaging and this argument is born out by practical experience. The chaotic zones near the 3/1 resonance are well described by the mappings; the size and shape of the chaotic zones are reproduced, as well as the Lyapunov exponent (Wisdom, 1983). However, we do not know of rigorous results which show that chaotic trajectories of averaged systems shadow trajectories of unaveraged systems for long time. Nevertheless, it is plausible that the chaotic trajectories of the mapping approximations are satisfactory representations of the chaotic trajectories in the modeled system. Proving numerical reliability is much more difficult in this case. Thus, especially in more complicated problems, it is not likely that we can rigorously prove the stability of the method, especially since each trajectory and stepsize must be considered individually. We can, however, hope to determine the borders and mechanisms of the gross instabilities through the application of the more heuristic tools of nonlinear dynamics such as the resonance overlap criterion for the onset of chaos.

We should not think of these possible artifacts as defects of the mapping method. The fact that the mapping method is itself a Hamiltonian system allows us to use the insight and methods of modern Hamiltonian dynamics to more clearly understand the issues of nonlinear stability, as well as these possible artifacts. Surely similar artifacts would appear in any finite difference scheme for solving a system of ordinary differential equations; for example, stepsize res-

onances have also recently been found in the family of symmetric integrators (Quinlan & Tremaine 1990; Quinlan & Toomre 1992).

4. STABILITY OF THE n-BODY MAPS

The Hamiltonian nature of our mapping method allows us to study the nonlinear stability of our mapping method using the usual tools of Hamiltonian dynamics. We propose that the principal instability of the mapping method is associated with an onset of chaos due to the overlap of resonances associated with the extra high-frequency terms introduced to generate the mapping. These resonances we call the stepsize dependent resonances. As usual in the analysis of the onset of chaos in a Hamiltonian system, we must first identify the principal resonances. We than calculate the location of each resonance and the width of the libration region associated with it. Chaos ensues if the principal resonance regions overlap. The resonance overlap criterion has been previously used in celestial mechanics to successfully predict the region of instability near the secondary in the restricted three-body body (Wisdom 1980; Duncan *et al.* 1989).

Resonances occur when linear combinations of the angular variables are slowly varying. When the Hamiltonian is written as a Poisson series in the angular variables, the most important resonances correspond to terms in the series with the largest coefficients. Writing the interaction Hamiltonian as a Poisson series in the Keplerian angle variables is the classical problem of the expansion of the disturbing function (e.g., Pierce 1849; Plummer 1960). An important property of this expansion is that the terms are proportional to various powers of the eccentricities and inclinations of the interacting planets; terms with arguments containing larger multiples of the longitudes of perihelion and longitudes of the ascending node are proportional to larger powers of the eccentricities and inclinations, respectively.

Expressing the mapping interaction Hamiltonian as a Poisson series is a straightforward extension of the usual expansion of the disturbing function. If we write the original interaction Hamiltonian as

$$H_{\text{Interaction}}=\sum_{\mathbf{i}}\beta_{\mathbf{i}}\cos(\mathbf{i}\cdot\boldsymbol{\theta}), \tag{11}$$

where $\boldsymbol{\theta}$ represents the full set of angle variables of the problem, and $\mathbf{i}$ is a vector of integers, $\mathbf{i}\cdot\boldsymbol{\theta}$ then represents a particular angular argument of the Poisson series, and $\beta_{\mathbf{i}}$ represents its coefficient in the sum. In the mapping, the interaction Hamiltonian is multiplied by delta functions. The interaction Hamiltonian becomes

$$2\pi\delta_{2\pi}(\Omega t)H_{\text{interaction}}=\sum_{\mathbf{i},l}\beta_{\mathbf{i}}\cos(\mathbf{i}\cdot\theta-l\Omega t). \tag{12}$$

That this equality holds may be seen by expanding the cosines of differences as a sum of a product of cosines and a product of sines. The sum over sines is zero because for every term with $l>0$ there is an equal but opposite term with $l<0$.

The most important resonances correspond to the terms in the Hamiltonian with the largest amplitudes. The largest terms in the expansion of the disturbing function are generally those with the smallest number of factors of the eccentricities and inclinations, since planetary eccentricities and inclinations are generally small. We consider only the lowest order terms. In the disturbing function itself there is only a single collection of terms which have no factors of eccentricity and inclination. The arguments of these terms are multiples of the difference between the mean longitudes of the pair of planets under consideration. These terms are not resonant except when the mean motions of the two planets are equal, but in this case the usual expansion of the disturbing function is not valid. Other terms in the expansion of the disturbing function are smaller because they are multiplied by various factors of the eccentricities and inclinations, but often are more important because in certain regions of the phase space their arguments can be slowly varying and there are large resonance effects. In the case of the mapping Hamiltonian, however, the terms in the disturbing function containing only pairwise differences of mean longitudes are now combined with multiples of the mapping frequency. The new combinations can be resonant. These are the dominant stepsize dependent terms in the mapping interaction Hamiltonian; they control the basic stability of the mapping method.

We analyze the resonances resulting from the stepsize dependent terms as we would any other Hamiltonian resonance. We write the resonance Hamiltonian as the unperturbed Hamiltonian plus those interaction terms corresponding to the resonances of interest. We presume for the moment that the nonresonant terms can be pushed to higher order by some suitable canonical transformation. In this analysis, we also ignore any physical resonances that may also exist in the system. Thus, the Hamiltonian governing the dominant stepsize dependent resonances is given by

$$H_{\text{Stepsize}}=H_{\text{Kepler}}-\sum_{0<i<j<n}\frac{Gm_im_j}{a_>}\times\sum_{k=0}^{\infty}\beta_k(\alpha)\sum_{l=-\infty}^{\infty}\cos[k(\lambda_i-\lambda_j)-l\Omega t], \tag{13}$$

where

$$\beta_k(\alpha)=\begin{cases}b^k_{1/2}(\alpha) & k>1,\\ b^k_{1/2}(\alpha)-\alpha & k=1,\\ \frac{1}{2}b^k_{1/2}(\alpha) & k=0.\end{cases} \tag{14}$$

The sum over i and j is a sum over distinct pairs of planets, the number of planets being $n-1$. The masses of the planets are m_i. The semimajor axes are a_i, $\alpha=a_</a_>$, $a_>$ is the larger of a_i and a_j, and $a_<$ is the smaller of the two. The sum over k gives the set of terms in the disturbing function which are independent of the eccentricities and inclinations, the coefficients of which are given in terms of the usual Laplace coefficients $b^k_s(\alpha)$, and the arguments of which depend solely on the pairwise differences of the

mean longitudes. There is a contribution from the indirect part of the disturbing function for $k=1$. The sum over l comes from the Fourier representation of the Dirac delta functions.

Resonances occur when one of the angular arguments is nearly stationary. In considering which resonances are important we must keep in mind that the mapping frequency is larger than all the orbital frequencies. We found empirically that the mapping method performed well provided that 10 or more mapping steps were taken for each orbit period. Thus the mapping frequency Ω is larger than all of the mean motions (the orbital frequencies) by a considerable factor. Stepsize resonances occur only if k is rather large. The coefficients are proportional to the Laplace coefficient $b^k_{1/2}(\alpha)$, which for small α is proportional to α^k. Terms with very high k are not as important as those with lower values of k. The most important stepsize resonances are those for which $l=\pm 1$. In any particular region of phase space, terms with larger $|l|$ have proportionately larger $|k|$

In the derivation of the mapping method we used canonical Cartesian Jacobi coordinates and conjugate momenta (see WH91). Resonance analysis is more easily carried out in some form of canonical Keplerian elements. The most convenient set for the present purpose is the set of modified Delaunay elements which have as coordinates the mean longitude, the longitude of pericenter, and the longitude of the ascending node (see Plummer 1960). Now our resonance Hamiltonian depends only on the mean longitudes, and the semimajor axes. The momentum conjugate to the mean longitude λ_i is $L_i=\sqrt{m'_i\mu_i a_i}$, where m'_i is the i^{th} Jacobi mass, which is nearly equal to m_i since the planetary masses are small, and $\mu_i=Gm_im_0$, where m_0 is the mass of the dominant central object. In terms of these canonical elements, the Keplerian Hamiltonian is

$$H_{\text{Kepler}}=-\sum_{i=1}^{n-1}\frac{m'_i\mu_i^2}{2L_i^2}. \tag{15}$$

In these variables, the Keplerian Hamiltonian is obviously integrable, since no angles appear.

Having identified the set of resonances of interest, we now analyze each in detail. For simplicity, we consider first only the terms for which $l=\pm 1$, the most important terms; the generalization to $|l|>1$ will be immediate. Thus for each pair of planets we consider each term in the sum over k separately. We call this the k^{th} stepsize resonance. For definiteness, we shall assume $n_i>n_j$, i.e., that $a_i<a_j$. The Hamiltonian for the k^{th} stepsize resonance for planets i and j is then

$$H_{ijk}=-\frac{m'_i\mu_i^2}{2L_i^2}-\frac{m'_j\mu_j^2}{2L_j^2}-\frac{Gm_im_j}{a_j}\beta_k(\alpha)\cos[k(\lambda_i-\lambda_j)-\Omega t]. \tag{16}$$

This resonance Hamiltonian contains only a single linearly independent combination of the angles. As usual we make a canonical transformation to a resonance variable which is this sole combination of angles. The transformation is carried out with a generating function of the form

$$F(\lambda_i,\lambda_j,\Lambda,\Sigma,t)=[k(\lambda_i-\lambda_j)-\Omega t]\Sigma+(c\lambda_i+d\lambda_j)\Lambda, \tag{17}$$

where the constants c and d are subject only to the constraint that $c\lambda_i+d\lambda_j$ be linearly independent from the combination $k(\lambda_i-\lambda_j)$. We arbitrarily choose $c=d=1$. The new angle variables are the resonance variable $\sigma=\partial F/\partial\Sigma=k(\lambda_i-\lambda_j)-\Omega t$ and the fast variable $\lambda=\partial F/\partial\Lambda=\lambda_i+\lambda_j$. The relationships among the momenta are $L_i=\partial F/\partial\lambda_i=\Lambda+k\Sigma$ and $L_j=\partial F/\partial\lambda_j=\Lambda-k\Sigma$. The new Hamiltonian is

$$H'_{ijk}=H_{ijk}+\frac{\partial F}{\partial t} \tag{18}$$

$$=-\frac{m'_i\mu_i^2}{2(\Lambda+k\Sigma)^2}-\frac{m'_j\mu_j^2}{2(\Lambda-k\Sigma)^2}$$

$$-\frac{Gm_im_j}{a_j}\beta_k(\alpha)\cos(\sigma)-\Omega\Sigma, \tag{19}$$

where a_j and α are assumed to be written in terms of the new momenta. This Hamiltonian now has only a single angle variable, σ, and is cyclic in λ. Thus the momentum conjugate to λ is an integral of the resonance Hamiltonian. The orbits of the conjugate pair (σ,Σ) can be determined simply by drawing contours of the resonance Hamiltonian H'_{ijk}, upon fixing the other constants.

Though the resonant motion is completely described by the contours of H'_{ijk}, it is instructive to study an approximation to it. We anticipate that the variations of the system away from exact resonance will be small. The resonance condition is that a difference of the mean motions of a pair of planets when multiplied by a relatively large integer is the mapping frequency. The fact that the coefficient β is small for large k suggests that only if the match of mean motions is rather good will there be any resonance effect. This will be confirmed by the following discussion. Thus, we assume the variations of Σ about some center Σ^* are small, and we expand the resonance Hamiltonian about this center. The σ dependent term is already small and to a good approximation it is well represented by its value at the resonance center. Define H_0 to be the σ independent terms

$$H_0=-\frac{m'_i\mu_i^2}{2(\Lambda+k\Sigma)^2}-\frac{m'_j\mu_j^2}{2(\Lambda-k\Sigma)^2}-\Omega\Sigma. \tag{20}$$

Now expand H_0 about the resonance center

$$H_0=H_0|_{\Sigma^*}+\left.\frac{\partial H_0}{\partial\Sigma}\right|_{\Sigma^*}(\Sigma-\Sigma^*)+\frac{1}{2}\left.\frac{\partial^2 H_0}{\partial\Sigma^2}\right|_{\Sigma^*}$$

$$\times(\Sigma-\Sigma^*)^2+\cdots. \tag{21}$$

The first term is a constant and can be ignored. The second term can be used to define the resonance center. At resonance the time derivative of σ is near zero. The time derivative of σ is given by Hamilton's equations as the derivative of the Hamiltonian with respect to Σ. Since the σ dependent term is small, the time derivative of σ is dominated by the derivative of H_0 with respect to Σ. Thus it is natural to define the resonance center Σ^* to be that point at which $\partial H_0/\partial\Sigma=0$. Variables evaluated at the resonance

center will be denoted by a superscript *. In more detail, the resonance center Σ^* is defined by

$$\left.\frac{\partial H_0}{\partial \Sigma}\right|_{\Sigma^*} = \frac{km_i'\mu_i^2}{(\Lambda+k\Sigma^*)^3} - \frac{km_j'\mu_j^2}{(\Lambda-k\Sigma^*)^3} - \Omega = 0. \quad (22)$$

Written in terms of the mean motions this resonance condition is just $k(n_i^* - n_j^*) - \Omega = 0$, as is easy to verify. As Λ is varied there is a continuous family of resonance centers. That there is a continuous family of resonance centers is easy to see: if for some n_i^* and n_j^* there is a resonance, then if both are increased by the same amount the resonance is maintained since the resonance condition depends only on their difference.

Returning now to the expansion of the resonance Hamiltonian about the resonance center, the linear term vanished through the definition of the resonance center. We are left with the quadratic term in $\Delta\Sigma = \Sigma - \Sigma^*$ and the σ dependent term

$$H_{ijk}' = \tfrac{1}{2}\gamma(\Delta\Sigma)^2 + \beta\cos(\sigma), \quad (23)$$

where the second derivative of H_0 is

$$\gamma = \left.\frac{\partial^2 H_0}{\partial \Sigma^2}\right|_{\Sigma^*} \quad (24)$$

$$= -3k^2\left[\frac{m_i'\mu_i^2}{(\Lambda+k\Sigma^*)^4} + \frac{m_j'\mu_j^2}{(\Lambda-k\Sigma^*)^4}\right], \quad (25)$$

$$= -3k^2\left[\frac{1}{m_i' a_i^{*2}} + \frac{1}{m_j^* a_j^{*2}}\right], \quad (26)$$

and β represents the coefficient of the σ dependent term

$$\beta = -\frac{Gm_i m_j}{a_j^*}\beta_k(\alpha^*). \quad (27)$$

The width of the resonance is determined by tracing the separatrix. For $\beta > 0$ and $\gamma < 0$, the unstable equilibrium is at $\Delta\Sigma = 0$ and $\sigma = 0$, so the value of the Hamiltonian on the separatrix is β. The resonance is widest at $\sigma = \pi$ at which point $\Delta\Sigma = 2\sqrt{\beta/\gamma}$. This width corresponds to the maximum deviation from the resonance center for which libration is allowed. In terms of the modified Delaunay variables the half width is $|\Delta L_i| = |\Delta L_j| = k\Delta\Sigma = 2k\sqrt{\beta/\gamma}$. Note that because of the constraint that $\Lambda = (L_i + L_j)/2$ is constant, the maximum of L_i corresponds to the minimum of L_j and vice versa. For small resonance widths we can approximate the width in $\alpha = a_i/a_j$ by $\Delta\alpha/\alpha = 2(\Delta L_i/L_i - \Delta L_j/L_j) = 2(1 + L_i/L_j)\Delta L_i/L_i$.

We have confirmed the existence of these stepsize resonances by computing the evolution of trajectories of a two planet system. To be specific, we chose the masses and semimajor axes to correspond to those of Jupiter and Saturn. We set the initial eccentricities and inclinations to zero to minimize the effect of physical resonances in the system. We then carried out a large number of short integrations (only 1000 iterations) with a large number of stepsizes and monitored the variations in energy. The resulting diagram (see Fig. 1) displays a resonance structure

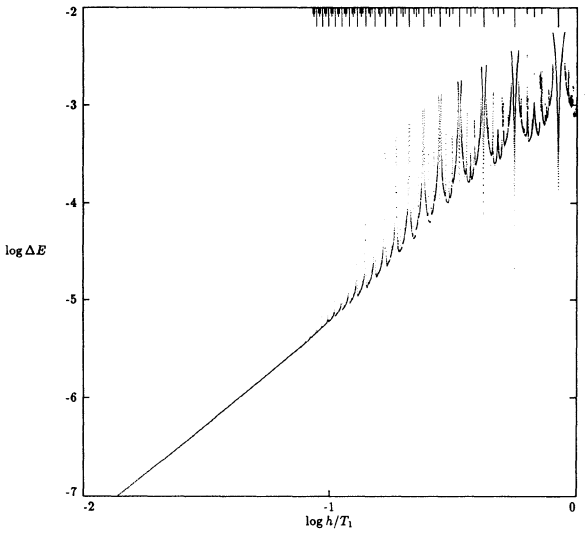

FIG. 1. The mapping exhibits stepsize resonances as predicted by the theoretical analysis. The points present observed short term relative energy variations for a large number of stepsizes. The lines at the top mark the location of the stepsize resonances in the region where the effect on the energy is greatest. Shorter lines correspond to higher order stepsize resonances.

which closely matches the predicted locations of the stepsize resonances. The relative energy variations are defined by $\Delta E = (E_{\max} - E_{\min})/(E_{\max} + E_{\min})$. Using this same system, we have also confirmed the detailed predictions of the analytical resonance analysis. We tuned the stepsize so that the system fell on the separatrix of the $k = 10$, $l = 1$ stepsize resonance. The resulting evolution is shown in Fig. 2. We plot the ratio of semimajor axes α versus the difference of mean longitudes of the two planets. We find a ten-lobed chain of islands, as expected. The width of each island, in

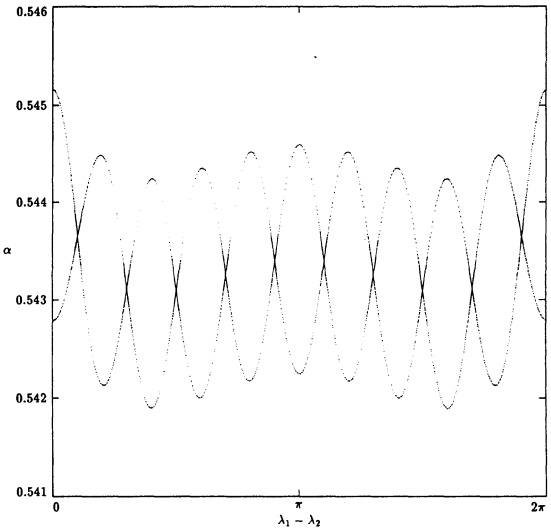

FIG. 2. The stepsize resonances have the width predicted by the theoretical analysis. The evolution of a trajectory near the separatrix of the $k = 10$, $l = 1$ stepsize resonance is shown.

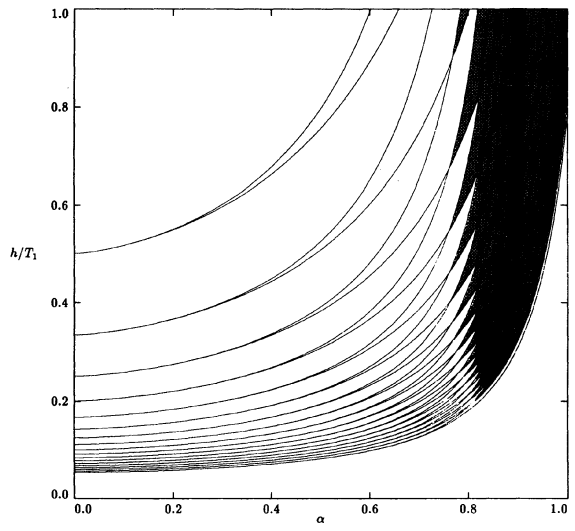

FIG. 3. The positions and widths of the stepsize resonances with $k \leqslant 30$, $l=1$. The infinity of resonances for larger k fall in the empty region in the lower right. For small α and h/T_1 the resonances get smaller faster than they accumulate. The region of resonance overlap is shaded. The overlap of resonances for α near 1 and moderate h is indicative of a real integrator instability.

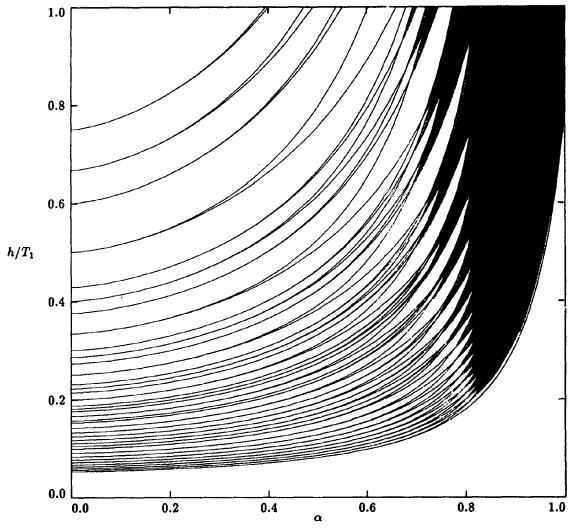

FIG. 4. The same as Fig. 3, but including stepsize resonances with $l<4$.

α, agrees with the above resonance analysis to better than one part in a thousand. Variables referring to the inner planet with the mass of Jupiter are denoted by subscript 1; those referring to the body with the mass of Saturn by a subscript 2. The initial conditions are $\alpha=0.54365$, $\lambda_1-\lambda_2=\pi/10$, to machine precision, and the stepsize is approximately given by $h/T_1=0.16701...$, where T_1 is the orbital period of our Jupiter. The semimajor axis of our Jupiter is $a_1=5.2$ AU, with $m_1=m_{\rm Sun}/1047.355$, and $m_2=m_{\rm Sun}/3501.0$. The length of the integration was about 20 000 years.

We now turn to the full ensemble of stepsize resonances. Figure 3 displays the positions and widths of the stepsize resonances for $k=2$–30, with $l=1$. There are an infinite number of resonances in the lower part of the figure for larger k. The stepsize resonances accumulate both near zero stepsize, and for α near 1. As the stepsize goes to zero the linear density of resonances is proportional to $1/k^2$, but the widths of these resonances decreases exponentially as $\alpha^{k/2}$. They decrease in size much more rapidly than they accumulate. Thus this region does not give resonance overlap. As expected, small stepsizes are stable. This large number of very small stepsize resonances corresponds to a subset of the multitude of small Poincare–Birkhoff islands we saw in the standard-map analogy given above. The accumulation of resonances as α approaches 1 is indicative of a real integrator instability. The widths increase as the stepsize gets larger, so for any α there is a critical stepsize above which the mapping method is unstable. In Fig. 4, we show the same diagram when resonances with $l<4$, and $k \leqslant 30$ are included. The higher order stepsize resonances fill in the gaps somewhat. Keep in mind that this figure has been computed for masses appropriate for the Jupiter–Saturn system; for other masses the diagram will be different.

We have tested the prediction of integrator instability in the region of resonance overlap, by computing the evolution of a large number of Jupiter–Saturn-like systems with various stepsizes and initial semimajor axis ratios. The grid of initial stepsizes and semimajor axis ratios is quite fine, with 100 values in each parameter. Thus 10 000 experiments were carried out. Each integration was continued up to the point of dissolution of the system, or for 100 000 years, whichever came first. The cumulative time spanned by these test integrations is of order one billion years. This test of the map would have been unthinkable without the speed of the mapping method. The results are shown in Fig. 5. In this figure a point is plotted if, during the integration, one of the planets became hyperbolic. Lyapunov exponents were also computed; the regions of rapid divergence of trajectories were essentially identical to the regions of gross instability. We see that the agreement of the unstable regions with the regions of resonance overlap is quite good. The tongues of instability that reach down from the right part of the diagram correspond well with the tongues of resonance overlap. Including higher order resonances and the chaotic width of the separatrices themselves would surely improve the agreement, but these are unnecessary refinements. The major instability is clear.

The experiment also reveals a second instability, unrelated to resonance overlap of the stepsize resonances, when the mapping stepsize is precisely half the orbital period of the innermost planet. Evidently, it is necessary for the stepsize to avoid low order commensurabilities so that the dynamics can accomplish a natural averaging over the orbit.

5. CONCLUSIONS

We have examined the stability of the new symplectic n-body maps from the point of view of nonlinear dynamics.

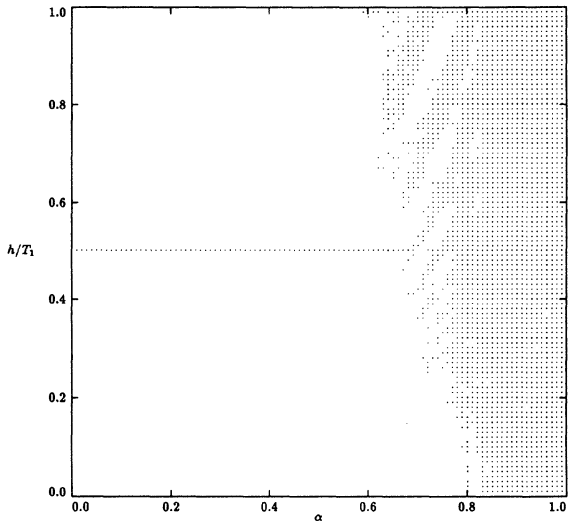

FIG. 5. Unstable integrations are indicated by a dot. The agreement with the predictions of the resonance overlap of stepsize resonances is quite good. The overlap of first order resonances of the real system accounts for the physical instability at small h for $\alpha > 0.8$.

We have identified the resonances responsible for the principal artifacts. These are resonances between the stepsize and the difference of mean motions between pairs of planets. For larger stepsizes resonant perturbations are evident in the variation of the energy of the system corresponding to these stepsize resonances. We have shown that the principal instability of the method can be predicted and corresponds to the overlap of the stepsize resonances. We note that the analysis suggests other artifacts will occur. For example, the overlap of a stepsize resonance with a resonance of the actual system may also give a region of chaotic behavior that is an artifact. We point out that the fact that the principal artifacts correspond to a particular set of stepsize resonances suggests that it may be possible to perturbatively remove the effect when the stepsize resonances are nonoverlapping (see Tittemore & Wisdom 1989).

This research was supported in part by the NASA Planetary Geology and Geophysics Program under Grant No. NAGW-706, by an NSF Presidential Young Investigator Award AST-8857365, and by an NSF Graduate Fellowship.

REFERENCES

Chirikov, B. V. 1979, Phys. Rep. 52, 263
Duncan, M., Quinn, T., Tremaine, S. D. 1989, Icarus 82, 402
Grebogi, C., Hammel, S., Yorke, J., & Sauer, T. 1990, Phys. Rev. Lett. 65, 1527
Laskar, J. 1989, Nature 338, 237
Lichtenberg, A. J., & Lieberman, M. A. 1983, Regular and Stochastic Motion (Springer, New York)
Percival, I. 1979, in Nonlinear Dynamics and the Beam-Beam Interaction, edited by M. Month and J. C. Herrera (AIP, New York).
Peirce, B. 1849, AJ, 1, 1
Plummer, H. C. 1960; An Introductory Treatise on Dynamical Astronomy (Dover, New York)
Quinlan, G. D. & Toomre, A. 1992, preprint
Quinlan, G. D. & Tremaine, S. D. 1990, AJ, 100, 1694
Sanz-Serna, J. M., & Vadillo, F. 1986, in Numerical Analysis, edited by D. F. Griffiths and G. A. Watson (Wiley, New York)
Sussman, G. J., & Wisdom, J. 1992 (submitted)
Tittemore, W., & Wisdom, J. 1987, Icarus, 74, 172
Wisdom, J. 1980, AJ, 85, 1122
Wisdom, J. 1982, AJ, 87, 577
Wisdom, J. 1983, Icarus, 56, 51
Wisdom, J., & Holman, M. 1991, AJ, 102, 1528 (WH91)